Enhancement efficiency of poly (o-toluidine) ZnO solar cells by using metal oxide-assisted poly (styrenesulfonate) poly (o-toluidine) poly (3,4ethylenedioxythiophene) nanostructures

Abdullah A. Hussein, Asrar Abdulmunem Saeed, Tahseen A. Alaridhee, and Fatima H. Malek

View Online   **Export Citation**

Enhancement Efficiency of Poly (o-toluidine) ZnO Solar Cells by Using Metal Oxide-Assisted poly (styrenesulfonate) poly (o-toluidine) poly (3,4ethylenedioxythiophene Nanostructures

Abdullah A. Hussein[1,a)], Asrar Abdulmunem Saeed[2], Tahseen A. Alaridhee[3] and Fatima H. Malek[1]

[1] *Department of Material Science, Polymer Research Centre, University of Basrah, Iraq.*
[2] *Department of physics, College of Science, Mustansiriyah University Iraq.*
[3] *Department of physics, College of Education for Pure Science, University of Basrah Iraq.*

E-mail of the corresponding author: [a)]amanar_2005@yahoo.com

Abstract. In this paper, we present the fabrication and the photo-physical characterization of a photovoltaic solar cell in the presence of Iron (III) oxide nanoparticles (Fe_2O_3 NPs). This latter is deposited at the hole's interface collecting the layer of buffer [poly(styrenesulfonate): poly(o-toluidine) and poly(3,4ethylenedioxythiophene) (PEDOT: PSS)] and (POT) Zinc Oxide Nanoparticle (ZnONPs) active layer. This additive at the interface was noticed to considerably elevate the performances of the solar cell. These devices' photo-physical characteristics are examined at the interface of POT: ZnONPs active layer and PEDOT: PSS buffer layer with Fe_2O_3 NPs with varied space distributions. The enhancement in optical characteristics occurs when the Fe_2O_3 NPs are appropriatley large to break through the active layer and subsequently improving the photovoltaic solar cells (PSCs) performances through hole collection efficiency gains. The hybrid PSCs considerably increases the power conversion efficiency (PCE) to 0.18% compared to 0.16% in conventional pure solar cells.

INTRODUCTION

As a low-cost and environmentally friendly power harvesting technology, getting electricity from of sunlight energy has become a very significant problem in latest years. A renewable source of energy for electrical energy was introduced by PSCs as an excellent technological potential. they represent a cheaper option to the common inorganic-based solar cells as they are compatible with flexible substrates and easily manufactured [1–6]. varied studies focused on improving the effectiveness of the PSCs and their fabrication methods. years ago, the studies focused on bulk-heterojunction (BHJ) photovoltaic cells which are made through mixing the n-type with the p-type p-conjugated polymer materials [7]. The significant enhancement of the PSCs' efficiency is still one of the most important topics nowadays.

There are four stages of converting the light into electricity which are: the absorption of light and the formation of exciton, exciton dissociation into free charge carriers, mobility of charge, and finally collection of charge by using the electrodes. the active materials' chemical structures affect these four stages, which are; donor (D) and acceptor (A), and the active polymer film morphology [8–10]. Due to the availability, high solubility in common organic solvents and high carrier mobility of The active layer (P3HT:PCBM), it is considered as a common organic acceptor and polymer donor for the organic photovoltaic cells. Huge progression has been noticed in the past few years on active layer (P3HT:PCBM) photovoltaic cells [10–12].

Although there is a huge number of studies and articles related to metallic nanoparticles (NPs) enhanced PSCs, the full knowledge of differences in the performance of photovoltaic cells remains unclear.. Many researches have

aproved the ability of improving the photoctive conjugated polymer absorption in the active layer by the plasmic scattering or near-field enhancement that is resulted from the effect of the metallic NPs localized surface plasmon resonant (LSPR) (mainly improves the optical properties) [13,14]. Also, Several studies have shown that the powerful near-field around the NPs is laterally distributed along the PEDOT: PSS layer due to the LSPR impact.. This results in light absorption improvement being decreased in the active layer. therefore, causing the enhancement of (PCE) in the expanded interface between and PEDOT: PSS buffer layer and the active layer in addition to the enhancement of the PEDOT: PSS conductivity (primarily improving the electrical property) [15]. Due to their low manufacturing costs, elevated absorption coefficient, and compatibility with flexible substrates, PSCs are very essential. the organic photovoltaic cells have some disadvantages, such as low efficacy, instability and short lifetime [16,17]. The objective of this research is to enhance effectiveness through enhancing absorption within an organic material. The latter is accomplished through integrating metallic nanoparticles within the absorbing layer and therefore producing surface plasmon. evanescent waves are produced by these surface plasmon through a powerful coupling between the electrons and an incident electromagnetic wave in the conduction band of a metal. This process happens once the frequency of both the incident wave and the plasmon resonant is equall. this results in a sharp rise in the electromagnetic field around metallic particles, enabling improved absorption in the surrounding medium. there are some factors that the resonant frequency differs accordingly which are; the given grating period, the material of the nanoparticlesand the surroundinng medium's optical constants [18]. In the visible spectrum, nanoparticles of metal oxide, silver and gold placed in free space each has its own resonant frequency. In this experiment, metal oxide nanoparticles were used. also, These nanoparticles' inclusion allows scattering of light, which in the   intermediate layer is particularly useful.

EXPERIMENT

Each glass substrate was washed in distilled water, isoproply alcohol and acetone, coated thoroughly by a transparent electrode of ITO (120nm thick, 15Ω/sq sheet resistance), dried by using nitrogen gas, heat dried, finally was treated for 10 minutes with cleaner of ozone-ultraviolet. The solution PEDOT: PSS (Sigma-Aldrich) is Mixed with Fe_2O_3NPs (50 nm and M.W=159). the Fe_2O_3NPs concentration in PEDOT: PSS   was 0.5 wt percent . Then, the solution has been spin-coated on the ITO substrate at (2000 rpm, 30 sec) which was pre-coated on the active layer surface. Thermal pre-annealing was performed on a dry oven in ambient air at 120 ° C for 30 minutes. At the moment of oxidative monomer polymerisation (o-toluidine), ZnONPs were added to the poly(o-toluidine) (POT) solution. The solution was stirred to disperse the NPs uniformly within the POT for 9 hours. The mixed solution of POT: ZnONPs was spin-coated on the PEDOT: PSS: Fe_2O_3NPs buffer layer in the air at (1000 rpm, 30 sec). The active layer's thickness is ~160 nm (by Elepsometry). As a cathode, Aluminium (Al ~50nm) was evaporated thermally following the photoactive layer spin-coating under a high vacuum of ~10^{-6} Pa with a 0.2 nm s^{-1} ratio onto the layer of the polymer. This leads to a device creation with an active area of 5mm^2 distinct through a shadow mask. The structure of the last device is ITO/PEDOT:PSS (Fe_2O_3NPs)/POT:ZnONPs/Al. the final stage, the completed photovoltaic cells' following the annealing process was continioued at 120 °C for 30 minutes inside a glove box.

CHARACTERIZATION

A computer-programmed Keithley 2400 source / meter was utilised to measure the devices' present density – voltage (J – V) characteristics, simulating the AM1.5 sunlight with a 100mW / cm^2 of energy density. for UV-vis absorption atomic force microscopy (AMF) and spectroscopy, spin coating POT: ZnONPs and PEDOT: PSS (Fe_2O_3NPs)glass substrates solution on glass substrates were used to prepare films. Varian Cary 5000UV (VIS-NIR) spectrometer was used to take the polymer films' UV-vis absorption spectra A regular photovoltaic (PV) reference cell calibrated the light intensity for the solar simulator. a Stanford 8300 lock-in amplifiern a Stanford lock-in amplifier 8300 unit was used to measure the curves of the external quantum efficiency (EQE). A BURKER NanoScope (I-V) Multimode adapter AFM with the tapping mode was used to acquire the polymer films' AFM images. Spectroscopic ellipsometry (M-2000) was used to measure the thickness of the film. The PCE (η) is described by η = FF× (Voc × Jsc)/P_{light}, where the FF is cell fill factor defined as F.F.=(I_{max} × V_{max})/(I_{sc}× V_{oc}) and P_{light} is the power of incident light.

RESULTS AND DISCUSSION

The PSCs photovoltaic characteristics with and without Fe_2O_3NPs were measured and compared with the purpose of examining the Fe_2O_3NPs plasmonic effects on the PSCs. First, the resulting of UV–vis absorption spectra is showen in Fig.1(a, b). Fig.1(a) presented the PEDOT:PSS layer's net absorption with the combined Fe_2O_3NPs has been gained. We can observe however that there was no improved absorption of light for the PEDOT:PSS layer has been obtained following coating by Fe_2O_3NPs. Conversely, Fig. 1 (b) shows that both of the films have characteristic peaks for POT in the 400–680nm range. Clearly, the UV–vis absorption peaks intensity slightly increases with Fe_2O_3NPs. One reason behind the enhancement in the generation of electron-hole pair in the active layer can be due to the dissipation of energy, that is appropriate to the electromagnetic field intensityLSPR. Another reason is the (LSPR) formation and the elevation of the light scattering because of the Fe_2O_3NPs usage, thus improving the efficiency of light absorption. The light is trapped inside due to the scattering of light that elongates the optical path in the active layer [19–22].

The presence of POT and ZnO were recorded and observed by XRD analysis. Fig.2 shows that ZnO were completely dispersed with the POT. Crystalline ZnO has the diffraction pattern displayed in Fig.2, where the reflections of planes (100), (002), (101), (102), and (110) correspond to as described the reported JCPDS data15 of the prepared NPs, and corresponding to peaks at 2= 31.41, 33.82, 36.42, 46.44, 56.47 and 62.9 plane, respectively [6].

The devices' present density (J) versus voltage (V) characteristics were measured and the results are shown in Fig 3. Table 1 showed the devices' characteristics. The fill factor was increased from 0.49 to 0.5, whereas the short-circuit current density (J_{sc}) and open-circuit voltage (V_{oc}) were increased from 0.74 to 0.78 mA.cm^{-2} and 0.46 to 0.48, respectively for the PEDOT:PSS/POT:ZnONPs photovoltaic cell and the PEDOT:PSS:Fe_2O_3NPs /POT:ZnONPs photovoltaic cell.
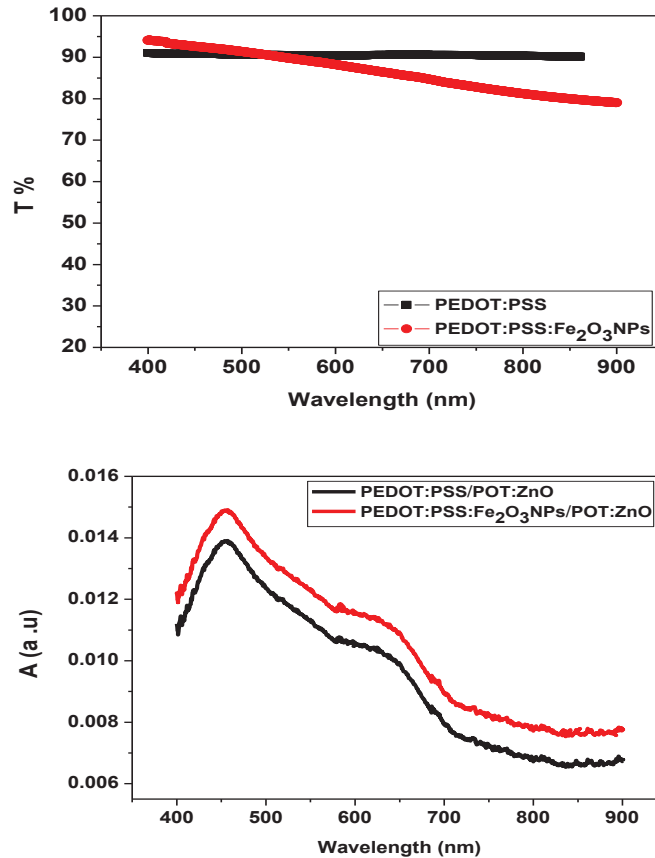
FIGURE 1.(a) UV–vis absorption spectra of PEDOT: PSS/POT: ZnO layer and (b) PEDOT: PSS :(Fe_2O_3)/ /POT: ZnO layer thin films.
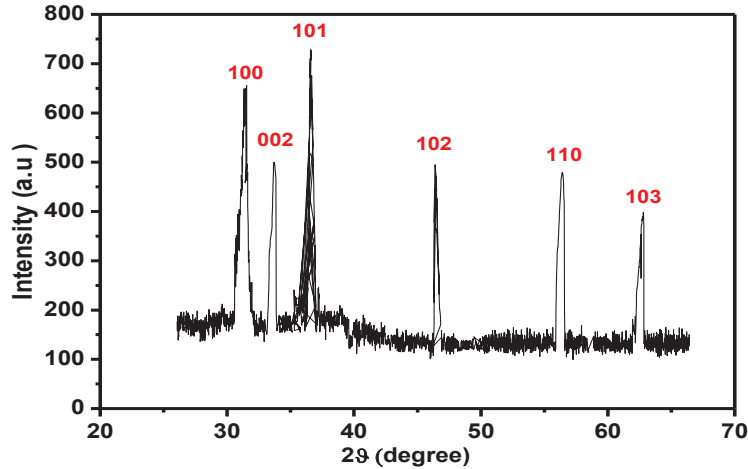
FIGURE 2. The XRD pattern of POT: ZnO active layer.

To obtain PEDOT:PSS:Fe_2O_3NPs /POT:ZnONPs PSCs with higher fill factor and current density, both hole and electron mobilities must be balanced and optimized. Thermal treatment annealing will more enhance the hole mobility in the PSCs and the hole is typically the highest mobility-carrier in polymer POT. The increased current density in PEDOT:PSS:Fe_2O_3 NPs/POT:ZnO photovoltaic cell compared to PEDOT:PSS/POT:ZnONPs photovoltaic cell can be because of the existence of inorganic Fe_2O_3NPs throughout the POT:ZnONPs active layer in hybrid film, that might elevate the mobility of charge carriers in the PEDOT:PSS:Fe_2O_3NPs/POT:ZnO photovoltaic cell. This increases the PCEof the PEDOT:PSS:Fe_2O_3NPs/POT:ZnONPs photovoltaic cell by up to (0.18%) compared to PEDOT:PSS/POT:ZnO photovoltaic cell PCE (0.16%).

To confirm this efficiency enhancement of the plasmonic PSCs, the incident photon-to-current conversion efficiency (IPCE) was measured. The IPCE for the and for the plasmonic PSCs and for the reference cell are shown in Fig.4. it is shown by the curves that there is an elevation in the EQE of PEDOT:PSS:Fe_2O_3 NPs device regarding to PEDOT:PSS device. in the photocurrent, There is a significant increase within the range of the wavelength from 400 to 900 nm following adding the Fe_2O_3NPs. These EQE data are in good agreement with the UV-vis data in Fig.2. also, in the broad range of the wavelength ,the device exhibited an improved quantum efficiency because of the light sofficient scattering. that shows a switching in the improvement of the optical absorption through the active layer close to the PEDOT:PSS:Fe_2O_3NPs buffer layer. It is recommended by the researchers that the improved plasmonic PSCs is basically resulted from the optical absorption elevation. This is because on the active layer, the incident light might be intensified because of the optical path elevation of incident light through the scattering from Fe_2O_3NPs and/or the Fe_2O_3NPs surface plasmons at resonant frequency.
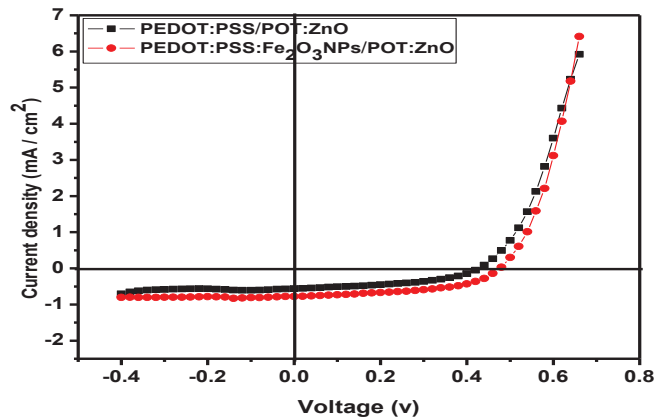
FIGURE 3. J–V curves of the solar cells fabricated with active layer/PEDOT: PSS layer and active layer/ PEDOT: PSS :(Fe_2O_3) thin films.

TABLE 1. Photovoltaic properties of the devices made with active layer/ PEDOT:PSS:(Fe$_2$O$_3$) thin films and active layer/PEDOT:PSS layer.

Device	J$_{sc}$(mA/cm^2)	PCE (%)	V$_{oc}$ (Volt)	FF
PEDOT:PSS/POT: ZnO	0.74	0.16	0.46	0.49
PEDOT:PSS:Fe$_2$O$_3$NPs/POT: ZnO	0.78	0.18	0.48	0.50
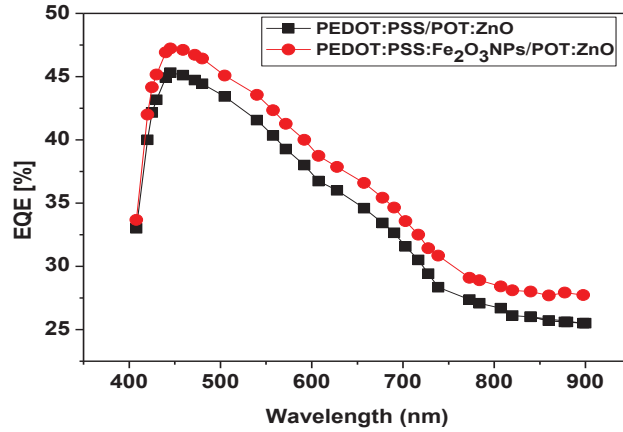
FIGURE 4. Incident photon-to-current conversion efficiency (IPCE) curves for the pristine and hybrid photovoltaic cells fabricated with PEDOT: PSS.

The morphology of the PEDOT:PSS/POT:ZnONPs and the PEDOT:PSS:(Fe$_2$O$_3$NPS)/POT:ZnONPs films were examined using AFM. With the purpose of understanding the devices' underlaying morphology in the last photovoltaic cells, by Al cathode removing from the last photovoltaic cells through the use of sticky tape, the samples were made, and the gained images of AFM are showed in Fig. 5. The root mean square (r.m.s) PEDOT:PSS film's roughness is 6.3nm. The roughness of the surface elevated to 6.9nm for the PEDOT:PSS: Fe$_2$O$_3$NPs film. The witnessed variation texture of the PEDOT:PSS:Fe$_2$O$_3$NPs thin film as well as the elevated roughness might be because of the existence of Fe$_2$O$_3$NPs in the PEDOT:PSS film that has experienced the process of annealing. The PEDOT:PSS:Fe$_2$O$_3$NPs film texture is uniform throughout the thin film surface [23].
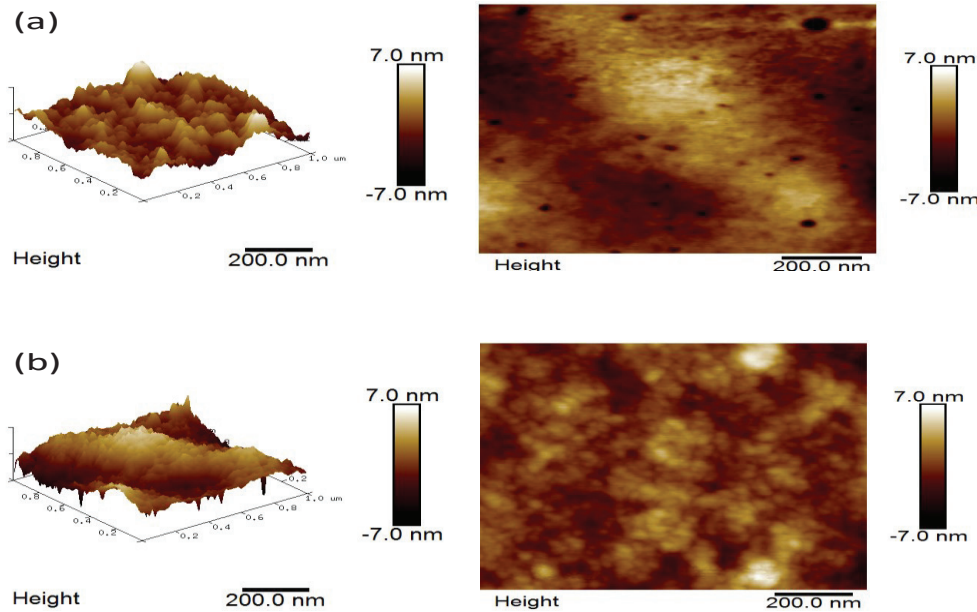
Figure.5. AFM images of the pristine PEDOT: PSS layer and hybrid PEDOT: PSS :(Fe$_2$O$_3$) layer thin films.

CONCLUSION

In this work, we fabricated good efficiency of PEDOT:PSS:Fe_2O_3 NPs hybrid photovoltaic cells by generating the Iron(III) oxide nanoparticles in PEDOT:PSS buffer layer, light harvesting system for PSCs of POT:ZnO. The device's light absorption varies with Fe_2O_3NPs and exhibited varied short-circuit current density (Jsc) because of the increased exciton generation. Fe_2O_3NPs contributed to the light harvesting increase. the charge-carrier[mobility in the hybrid PSC is increased because of The existence of Fe_2O_3NPs. We expect that this innovative and new notion of creating hybrid polymer fullerene:inorganic PSCs will be usefull with the purpose of enhancing the polymer PSCs power conversion efficiency even further in the near future.

ACKNOWLEDGMENTS

REFERENCES

1. C.J. Brabec, N.S. Sariciftci, J.C. Hummelen, Advan. Funct. Mater. **11**, 15 (2001).
2. H. Spanggaard, F.C. Krebs, Sol. Energy Materi. Sol. Cells **83**, 125 (2004).
3. K.M. Coakley, M.D. McGehee, Chem. Mater. **16**, 4533 (2004).
4. R.A.J. Janssen, J.C. Hummelen, N.S. Sariciftci, MRS Bull. **30**, 30 (2005).
5. E. Bundgaard, F.C. Krebs, Sol. Energy Mater. Sol. Cells **91** 954 (2007).
6. S. Gü nes, H. Neugebauer, N.S. Sariciftci, Chem. Rev. **107**, 1324 (2007).
7. G. Yu, J. Gao, J.C. Hummelen, F. Wudl, A.J. Heeger, Science **270**, 1789 (1995),
8. H. Hoppe, N. S. Sariciftci, J.Mater.Chem.**16**, 45–61 (2006).
9. E. Bundgaard, F. C. Krebs, Sol. Energy Mater.Sol.Cells **91**, 954–985 (2007).
10. S. Gunes, H. Neugebauer, N. S. Sariciftci, Chem.Rev.**107**, 1324–1338 (2005),
11. J. H. Hou,Z. A. Tan, Y. Yan,Y. J. He, C.H.Yang,Y.F.Li, J. Am. Chem. Soc.**128**, 4911–4916 (2006).
12. C.S hi,Y.Yao,Y.Yang,Q.Pei, J.Am.Chem.Soc.**128**, 8980– 8986 (2006).
13. J. L. Wu, F. C. Chen, Y. S. Hsiao,F.C.Chien,P.Chen,C. H. Kuo, M. H. Huang, C. S. Hsu, ACS Nano **5**, 959–967 (2011).
14. J.Yang, J. B.You, C. C. Chen, W. C. Hsu, H. R. Tan, X. W. Zhang, Z. R.Hong,Y.Yang, ACSNano **5**, 6210–6217 (2011).
15. D. D. S. Fung,L. F. Qiao,W.C.H.Choy, and C.Wang,W.E.I.Sha,F.X.Xie,S.L.He, **21**, 16348–16356 (2011).
16. M. Jørgensen, K. Norrman, and F. C. Krebs, Sol. Energy Mater.Sol.Cells **92**, 686–714. (2008).
17. F. C. Krebs, M. Jørgensen, K. Norrman, O. Hagemann, J. Alstrup, T. D. Nielsen, J. Fyenbo, K. L arsen, and Jette Kristensen, Sol. Energy Mater. Sol. Cells **93**, 422–441 (2009).
18. K. L. Kelly, E. Coronado, L. L. Zhao, and G. C. Schatz ,J. Phys. Chem. B **107**, 668 – 677 (2003).
19. S. A. Maier, H A. Atwater, J. Appl. Phys. **98**, 101 - 111 (2005).
20. B. P. Rand, P. Peumans, and S. R. Forrest, J. Appl. Phys. **96**, 7519-7526 (2004).
21. F. Monestier, Solar Energy Material. Solar Cells, **91**, 405-410 (2007).
22. E. K .Park, M. Choi, J.H. Jeun, K.T. Lim, J. M.Kim, and Y.S. Kim, Microelectronic Engineering **111**, 166–169 (2013).
23. H. Nguyen, H. Hopee, T. Erb, S. Gunes, G. Gobsch and N.S. Sariciftci, Adv. Funct. Mater. **17**, 1071 (2007).